LIMIT CYCLE OSCILLATIONS OF A VIOLIN STRING

B Shayak

Department of Theoretical and Applied Mechanics,
Sibley School of Mechanical and Aerospace Engineering,
Cornell University,
Ithaca – 14853,
New York State, USA

sb2344@cornell.edu shayak.2015@iitkalumni.org

Classification

PACS : 46.40.-f 05.45.-a

Keywords : Partial differential equation Limit cycle oscillations Stick-slip friction

Abstract

In this work we write and solve a first principles model for the motion of a bowed string. We find limit cycle oscillations driven by stick-slip friction. The shape of these oscillations is in accordance with the Helmholtz-Rayleigh motion. We observe that when bow force, bow speed and other parameters are varied, the stable limit cycle occurs in a narrow region of parameter space. This explains why it is difficult for amateurs to produce musically acceptable sounds from the instrument.

Lead paragraph

The problem of motion of a bowed string (violin, viola, cello and similar instruments) has intrigued scientists from more than a century. Most researches are derivatives of Rayleigh's original study, where he obtained solutions of the wave equation by making a starting assumption regarding the form of the motion.

We propose a model which quantitatively incorporates the stick-slip friction at the outset. The motion of the string is governed by the wave equation, while stick-slip friction at the bow point introduces a nonlinearity. By piecewise solution of the wave equation in the stick and slip phases, we obtain the solution of the nonlinear system. Our framework allows us to freely vary parameters such as bow point and bow force and determine the motion in each case.

Introduction

The problem of analysing the motion of a bowed string has been around for 140 years. The earliest attempt to understand the motion was by Helmholtz, whose observations were quantified and systematized by the Lord Rayleigh [1]. He has solved the homogeneous wave equation after making the assumption (on the basis of Helmholtz's observations) that the velocity of each point of the string is constant upwards for part of the time and constant downwards for the remainder of the time. This assumption incorporates the stick-slip friction – there is only vague and qualitative justification as to why that friction should give rise to such a motion. A more elaborate follow-up calculation, using D'Alambert's formula instead of eigenfunction expansion, was done by Raman [2] but again the Helmholtz type motion is taken as a starting point. The model was yet further amplified and compared with experiments by Schelleng [3,4] while a summary of literature may be found in Woodhouse [5-7]. In one of these papers, Woodhouse has also presented an insightful discussion of the transients leading to the limit cycle motion. A different approach has been adopted by Keller [8]. He has started from a first-principles model with a realistic treatment of the friction characteristics. The analytical development, using D'Alambert's formula, is extremely complex and the end result is that a solution has been obtained only for the case where the string is bowed at its midpoint.

Here, we write a first-principles model like Keller but for solution use eigenfunction expansions like Rayleigh. Further, we bring to bear the powerful method of matched boundary conditions to obtain the motions of the string. Our approach yields the limit cycle Helmholtz-Rayleigh motion as an output rather than an input. It also yields the regions of parameter space where the limit cycle occurs. Such a study has not been performed in the prior works – in Reference [1] and its derivatives the friction or the bow motion do not appear explicitly in the equations. In Reference [8], there is an attempt on stability analysis for the string bowed at its midpoint. The conclusion is that there is a loss of stability if and only if there exists a sufficiently high bowing velocity where the friction between string and bow increases with increase in velocity – otherwise the periodic motion is stable for all bowing force and speed. This is not fully in accordance with the practical observation that the violin is difficult to play, and any incorrect technique results in undesirable sounds being emitted from the instrument.

From a dynamical systems perspective, the present study is one of the first papers that we are aware of where a limit cycle in a PDE system has been analytically characterized. For example, in References [10-12], limit cycles have been shown in systems which are technically governed by PDEs, but actually have been modelled as ordinary differential equations (ODEs) by the authors. In Reference [13], a PDE effect is observed to destabilize a limit cycle present in an ODE system. In Reference [14], a PDE system does show a limit cycle but the same has not been characterized analytically due to extreme complexity of the system.

The outline of this article is as follows. In Section 1 we derive the equation of motion of the string. In Section 2 we solve the equation by obtaining the Fourier coefficients on a computer. In Section 3 we present some features of the solution. We conclude with a discussion.

1. Formulation of equation of motion

Stick-slip friction refers to the commonly observed phenomenon that the coefficient of kinetic friction between two bodies in contact with each other is less that that of static friction. This can lead to interesting kinds of oscillatory phenomena. A simple example may be found in Stoker [15]. This apparatus consists of a block of mass m attached to a spring of constant k and mounted on a conveyor belt moving with speed v_0. Stick-slip friction acts between the mass and the belt. The coefficient of static friction is μ_s while that of kinetic friction is μ_k with $\mu_k<\mu_s$.

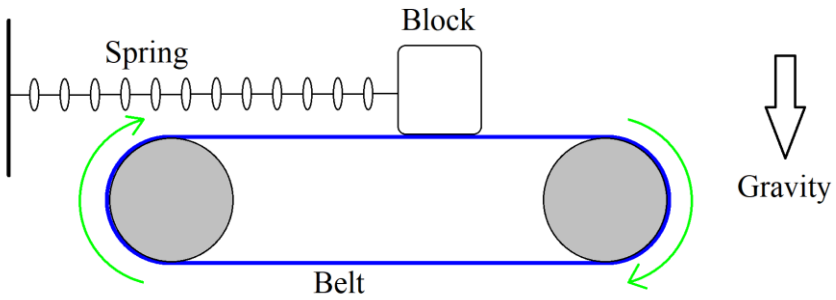

Figure 1 : Spring-mass-belt system which shows stick-slip friction driven limit cycles.

The analysis of the motion can be simplified if one makes the assumption that $\mu_k=0$. In this case, the qualitative nature of the motion is apparent. One starts from

a time when the mass is moving with the belt with the spring force being balanced by the static friction force. Evidently, this motion state will continue until the extension of the spring becomes equal to $\mu_s mg/k$. Beyond this point, the mass will start to slip. Since μ_k=0 by the assumptions, the dynamics will now be that of the spring and mass alone. This motion will continue until the mass acquires at some point in its trajectory the velocity v_0 of the conveyor belt. At this time, it will become at rest relative to the belt and static friction will come into effect, causing the cycle to start over again.

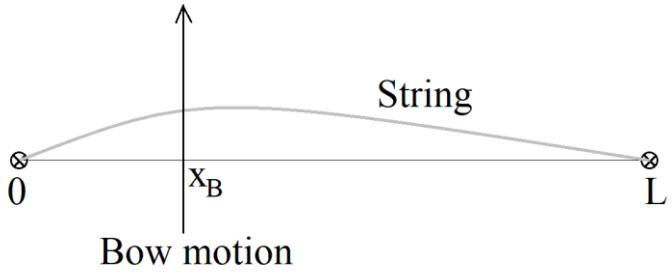

Figure 2 : Schematic representation of the violin string.

We extend this logic to the violin string. We consider the string as shown in the Fig. 2. It is tuned to a constant tension T and clamped at the two ends x=0 and x=L. The displacement $y(x,t)$ of the string satisfies the damped 1+1 wave equation

$$\frac{\partial^2 y}{\partial x^2} = \frac{1}{c^2}\frac{\partial^2 y}{\partial t^2} + \gamma \frac{\partial y}{\partial t} \quad , \tag{1}$$

with the damping constant γ being very small. The bow is drawn across the string at the point x=x_B with constant velocity v_0. It applies a concentrated force (delta function line load) F at x_B, perpendicular to the plane of the page. The friction between the bow and the string is stick-slip with the static value being μ_s and the kinetic value again being assumed to be zero.

To obtain the motion of the string, we will start tracking the state of the system at the point where the string just transitions from a stick phase to a slip phase of motion. From this point onwards, its displacement satisfies the homogeneous wave equation. It enters the stick phase when the velocity of the bow point becomes equal to that of the bow. During this phase, the point x=x_B moves upwards with constant velocity v_0, and the two parts to its left and right can be assumed to satisfy the wave equation separately. The stick phase ceases when the

normal component of tension at $x=x_B$ exceeds the friction force, and the next cycle of motion begins at this time.

Thus, by analogy with the spring-mass-belt system, we have constructed the equation of motion of the bowed string. In the next section we will see how to solve this equation.

2. Solution of the equation of motion

As a preparation for our primary objective, we first solve the spring-mass-belt system. Letting x be the displacement of the mass from the equilibrium point of the spring, the stick→slip transition occurs and the slip phase starts when the inward force of the spring balances the restoring force of friction i.e. at $x=x_0=\mu mg/k=\mu g/\omega^2$ (where μ is the coefficient of static friction, since we are assuming the kinetic coefficient to be zero, and ω is of course the natural frequency of the system). At this time, it is moving with the belt so its velocity is v_0. Letting $t=0$ be the start of slip, the solution during slip is evidently $x = x_0 \cos\omega t + (v_0/\omega)\sin\omega t$ which we can rewrite as

$$x = \left(x_0^2 + \frac{v_0^2}{\omega^2} \right)^{1/2} \cos\left(\omega t - \varphi\right) \quad , \tag{2}$$

where $\varphi=\arctan(v_0/\omega x_0)$.

The slip→stick transition occurs when the velocity of the mass becomes equal to v_0 i.e. the block becomes are rest relative to the belt. So we first calculate the velocity by differentiating (2). Letting t_1 be the time when this equals v_0, we get

$$\sin\left(\omega t_1 - \varphi\right) = -\frac{v_0}{\left(\omega^2 x_0^2 + v_0^2\right)^{1/2}} \quad .$$

Plugging this into (2) and simplifying,

$$x(t_1) = \pm\left(x_0^2 + \frac{v_0^2}{\omega^2} \right)^{1/2} \left(1 - \frac{v_0^2}{\left(\omega^2 x_0^2 + v_0^2\right)^2} \right)^{1/2} \quad . \tag{3}$$

The positive root is an unphysical solution and the negative root is the actual solution for $x(t_1)$. At this point, the block sticks to the belt.

We have now described the motion of the block completely. When slip starts, it evolves as per (2) from the point x_0 to the point x_1 which is given by (3). It then sticks to the belt and gets carried by it out to the point x_0 at uniform velocity v_0. Then, it starts slipping again and the cycle begins afresh. The trajectory $x(t)$ of the periodic state thus looks like a portion of a sinusoidal curve joined to a straight line. Further quantitative analysis of the condition (3) and the resulting amplitude and period of motion under various limiting cases is no longer of interest but we note that the analysis requires a matching of the slip and stick solutions.

Now we come to the violin. We will use separation of variables to solve the PDE. The solution of the damped wave equation with double zero boundary conditions at $x=0$ and $x=l$ (the more usual L is the length of the violin string here, while this analysis is general) is

$$y(x,t) = \sum_n \sin\frac{n\pi x}{l} \mathrm{e}^{-\gamma t/2} \left(A_n \cos\omega_{dn} t + B_n \sin\omega_{dn} t \right) \quad , \tag{4}$$

where the n^{th} damped frequency is

$$\omega_{dn} = \frac{\sqrt{\frac{4n^2\pi^2c^2}{l^2} - \gamma^2}}{2} \quad . \tag{5}$$

Because the damping is light, we will let ω_{dn} be equal to $n\pi c/l$, ignoring the correction. Then, pulling the decaying exponential outside the summation, we have

$$y(x,t) = \mathrm{e}^{-\gamma t/2} \sum_n \sin\frac{n\pi x}{l} \left(A_n \cos\frac{n\pi c t}{l} + B_n \sin\frac{n\pi c t}{l} \right) \quad . \tag{6}$$

Going further with the light damping approximation, we shall say that the velocity profile is

$$\dot{y}(x,t) = \mathrm{e}^{-\gamma t/2} \sum_n \sin\frac{n\pi x}{l} \left(-\frac{n\pi c}{l} A_n \sin\frac{n\pi c t}{l} + \frac{n\pi c}{l} B_n \cos\frac{n\pi c t}{l} \right) \quad , \tag{7}$$

where we neglect terms order $\gamma/(n\pi c/l)$, which is typically 1 percent for the lowest frequency and is still smaller for the higher harmonics. We note that the damping is not an essential phenomenon in the dynamics. As we saw for the mass-spring-belt example, the damping was not required to drive the mass into the limit cycle – the stick-slip friction automatically kills off the homogeneous motions. We are not taking $\gamma=0$ here so that spontaneous oscillations of the violin string, which occur when the bow is not coupling to it, die off in time. Then, we can easily tell

these motions apart from the limit cycle and also prove the role of the friction in providing the energy for driving the oscillations.

Given this, we now have the Fourier formulae – if at t=0 the initial position be $f(x)$ and the initial velocity be $g(x)$ then

$$A_n = \frac{2}{l}\int_0^l f(x)\sin\frac{n\pi x}{l}\,\mathrm{d}x \quad , \tag{8a}$$

$$B_n = \frac{2}{n\pi c}\int_0^l g(x)\sin\frac{n\pi x}{l}\,\mathrm{d}x \quad . \tag{8b}$$

This completes the presentation of the basic tools required for our analysis.

Now we come to the violin string itself. Suppose that a phase of slip starts at some time $t=t_0$. From this time onwards, the string as a whole satisfies the damped wave equation. We can write the displacement as

$$y^{(1)} = \sum_n \sin\frac{n\pi x}{L}\,\mathrm{e}^{-\gamma(t-t\_0)/2}\left(C_n\cos\frac{n\pi c\left(t-t_0\right)}{L} + D_n\sin\frac{n\pi c\left(t-t_0\right)}{L}\right) \quad , \tag{9}$$

where the superscript (1) refers to the slip phase and the C_n's are D_n's are all unknown. The long-term objective of our analysis will be to determine a relation between the C_n's and D_n's at the start of one phase of slip, and those at the start of the next.

Just as for the block, slip continues until a time t_1 when the velocity of the string at the bow point x_B becomes identically equal to v_0. Thus, the condition for transition from slip to stick is

$$\dot{y}^{(1)}\left(x_B,t_1\right) = v_0 \quad . \tag{10}$$

The dynamics in the stick phase is more interesting. Here, the bow drags the point $x=x_B$ at constant speed v_0. If $y^{(1)}(x_B,t_1)=y_1$ (a quantity which comes out when checking for the slip→stick transition), then the subsequent motion of this point is $y^{(2)}(x_B,t)=y_1+v_0(t-t_1)$, where the superscript (2) denotes the stick phase.

To find the motion of the rest of the string, we split it up into two parts – one running from 0 to x_B and one from x_B to L. We let L_1 and L_2 (=L–L_1) denote the lengths of these two segments (of course L_1 and x_B are numerically equal, but their connotations are different – L_1 is the length of the sub-string while x_B is the coordinate of the bow). Because one boundary point of each sub-string is moving, they will both satisfy an inhomogeneous wave equation rather than the

homogeneous one, and the general solution will be a particular or steady state solution on top of the homogeneous motions.

The steady state solution for each sub-string is a rotation about its respective clamp at constant angular velocity. For the left sub-string, this rotation is

$$y_{ssL}^{(2)} = \frac{\left(y_1 + v_0(t-t_1)\right)x}{L_1} \quad , \tag{11}$$

(subscript L denotes left) and its derivative is

$$\dot{y}_{ssL}^{(2)} = \frac{v_0 x}{L_1} \quad . \tag{12}$$

For the right sub-string, the steady state displacement is the straight line connecting the point (x_B,y_1+v_0(t–t_1)) to the point (L,0). We have

$$y_{ssR}^{(2)} = \left(y_1 + v_0(t-t_1)\right)\left(1 - \frac{x-x_B}{L_2}\right) \quad , \tag{13}$$

and its derivative

$$\dot{y}_{ssR}^{(2)} = v_0\left(1 - \frac{x-x_B}{L_2}\right) \quad , \tag{14}$$

and the steady state solutions of the two sub-strings have been determined.

If we subtract off the particular solutions, then the remaining motions exhibited by the sub-strings are just solutions of the damped wave equation with double zero boundary conditions. Hence they satisfy the relations (4-7) with the length being L_1 and L_2 as appropriate, and the initial time being t_1 instead of zero. So we can write

$$y_L^{(2)}(x,t) = y_{ssL}^{(2)} + \mathrm{e}^{-\gamma(t-t\_1)/2}\times \sum_n \sin\frac{n\pi x}{L_1}\left(E_n \cos\frac{n\pi c\left(t-t_1\right)}{L_1} + F_n \sin\frac{n\pi c\left(t-t_1\right)}{L_1}\right) \quad . \tag{15}$$

For the right sub-string,

$$y_R^{(2)}(x,t) = y_{ssR}^{(2)} + \mathrm{e}^{-\gamma(t-t\_1)/2}\times \sum_n \sin\frac{n\pi\left(x-x_B\right)}{L_2}\left(G_n \cos\frac{n\pi c\left(t-t_1\right)}{L_2} + H_n \sin\frac{n\pi c\left(t-t_1\right)}{L_2}\right) \quad . \tag{16}$$

Finally we have to evaluate the coefficients E_n to H_n. These come from the continuity of y and $\partial y/\partial t$ at the transition from slip to stick. For the left sub-string, the initial position and velocity are $y_L^{(1)}(x,t_1)$ and $\dot{y}_L^{(1)}(x,t_1)$, while for the right sub-string they are $y_R^{(1)}(x,t_1)$ and $\dot{y}_R^{(1)}(x,t_1)$, where by the L and R subscripts we now understand the portions of the original string in the two intervals [0, x_B] and [x_B, L].

Since there is a steady state solution, the eigenfunction expansion is performed upon the initial condition minus the steady state solutions evaluated at $t=t_1$. This then gives

$$E_n = \frac{2}{L_1}\int_0^{L_1}\left(y_L^{(1)}(x,t_1) - y_{ssL}^{(2)}(x,t_1)\right)\sin\frac{n\pi x}{L_1}\,\mathrm{d}x \quad , \tag{17a}$$

$$F_n = \frac{2}{n\pi c}\int_0^{L_1}\left(\dot{y}_L^{(1)}(x,t_1) - \dot{y}_{ssL}^{(2)}(x,t_1)\right)\sin\frac{n\pi x}{L_1}\,\mathrm{d}x \quad , \tag{17b}$$

for the left sub-string and

$$G_n = \frac{2}{L_2}\int_0^{L_2}\left(y_R^{(1)}(x,t_1) - y_{ssR}^{(2)}(x,t_1)\right)\sin\frac{n\pi x}{L_2}\,\mathrm{d}x \quad , \tag{18a}$$

$$H_n = \frac{2}{n\pi c}\int_0^{L_2}\left(\dot{y}_R^{(1)}(x,t_1) - \dot{y}_{ssR}^{(2)}(x,t_1)\right)\sin\frac{n\pi x}{L_2}\,\mathrm{d}x \quad , \tag{18b}$$

for the right.

We now ask for the time when the stick solution goes back to slip. The block performed this transition when the spring pulled it so hard that the friction could not keep up with it. Here, the force which will oppose the friction is the tension. Dragging the bow point will create a kink in the string – the greater the displacement of the bow point, the more pronounced the kink. A kink means a discontinuity in the derivative y' at $x=x_B$. The normal component of tension is of course $T\sin\theta$ which is Ty' – a jump in the derivative will give rise to a macroscopic contribution at the bow point. The bow point will stick so long as this force remains less than the friction, which is μF where F is the bow force. Thus, the condition for stick going to slip is

$$T\left(y_L^{(2)}{}'(x_B,t_2) - y_R^{(2)}{}'(x_B,t_2)\right) = \mu F \quad . \tag{19}$$

This of course defines the time of transition as t_2.

Now, the desirable quantities are the coefficients C_n and D_n at the time t_2 which is the start of the next phase of slip. As usual, the transition will be constrained by continuity of position and velocity at $t=t_2$. We already have the stick solution (15-18) at t_2; now we have to choose the coefficients C_n and D_n such that plugging them into (9) with t_0 replaced by t_2 produces a new slip solution which obeys the required ICs at $t=t_2$. Evidently,

$$C_n = \frac{2}{L}\int_0^L y(x,t_2)\sin\frac{n\pi x}{L}\,\mathrm{d}x \quad , \tag{20a}$$

$$D_n = \frac{2}{n\pi c}\int_0^L \dot{y}(x,t_2)\sin\frac{n\pi x}{L}\,\mathrm{d}x \quad , \tag{20b}$$

and we have obtained the required relation between the C_n's and D_n's at the start of one cycle and that of the next.

3. Results

The algorithm we presented above is analytically impossible to solve but computationally simple. Hence we write a program to implement it. We partition space into 300 points including boundaries, and initialize the first 60 spatial eigenfunctions. The numbers 60 and 300 were chosen because it was found that they generate accurate time traces in reasonable time-frames. There is no perceptible change in the time trace when the size is increased, so long as the number of harmonics and the number of spatial points considered are both increased in proportion. More on this will be discussed later. We then initialize the arrays for C_n to H_n, all of size 60 (i.e. the array C equals [C_1; C_2; …..; C_{60}] etc). We also initialize the arrays y and y_d (which is $\partial y/\partial t$) both of size 300 (same size as the x-array) and create a variable called mode whose value 1 denotes slip and 2 denotes stick.

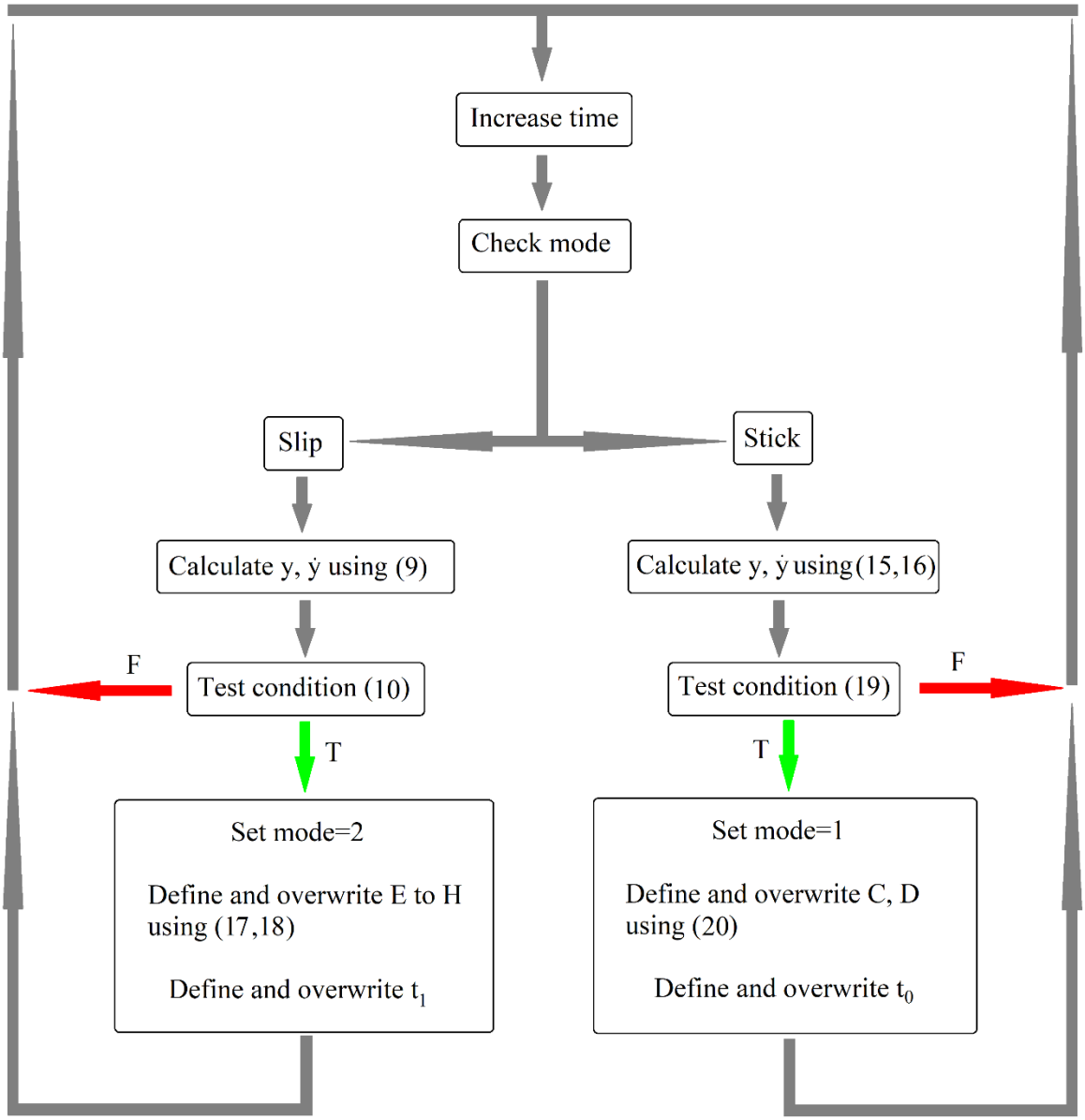

Figure 3 : Flow chart for the computation of the solution.

To run the program we loop over the variable t which starts from zero and increases with each iteration. Since the lowest natural frequency of the string turns out to be approximately 300 Hz, a time incrementation of 10^{-5} s at each step has been adopted. The following initial conditions are chosen : $y(x,0)$ consists of two straight lines between the clamps and the bowing point, with the displacement at x_B having the value 1/16500, and $\dot{y}(x,0)=0$. The choice of this IC is motivated by the fact that for x_B=1/3, this amounts to an exact satisfaction of the transition from stick to slip, while for other x_B it is sufficiently close to such

a transition that the system goes into the limit cycle oscillation. This condition determines the initial C_n's while D_n to H_n are trivial. The initial mode is 1 (slip) while $t=t_0=0$. At every t we calculate the elements of the array y and y_d (which are of the same size as x), use these to check for conditions and continue the solution.

The central block of the program implements the following algorithm, which is presented as a flow chart in Fig. 3. We now present the output of the program. The parameters are all as specified in the question. The first plot considers $x_B=L/3$ i.e. the bow point is taken as lattice site #100. The bow speed is $v_0=0.06$. The output is the curve of $y(x,t)$ with x corresponding to lattice site #81. Time is measured in seconds and displacement in mm (conventions which will be used in all plots).

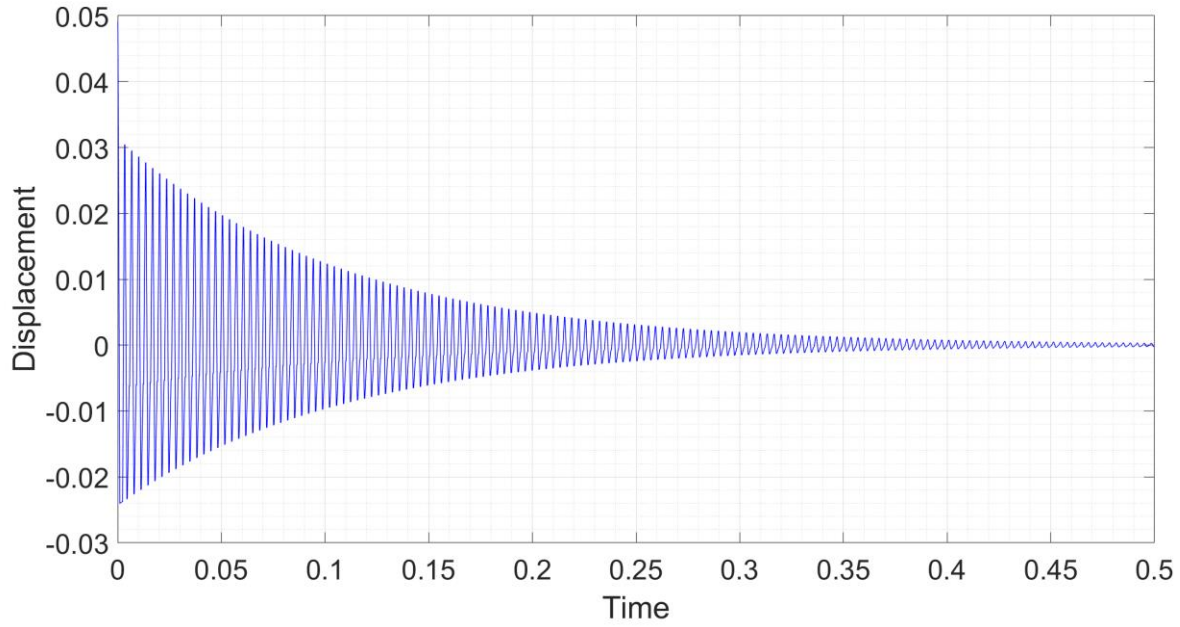

Figure 4 : Time trace of oscillations for excessively slow bow movement, when the bow does not couple.

We can see that the oscillations are damped. These are generated by the IC and not by the bow, showing that the bow has not coupled to the string. (The absence of γ in the equations would have resulted in an undamped oscillation here, making it difficult to recognize the bow-driven limit cycle when it occurs.) Raising the bow speed to 0.08 produces the limit cycle. The cycle persists in the range of bow speed from about 0.07 to 0.09 – it again disappears when $v_0=0.1$. The amplitude of the limit cycle increases initially upto a maximum at about $v_0=0.085$; it then

drops and the cycle eventually vanishes. If the bow point is relocated to #50, then also we get a similar behaviour, with the limit cycle motion appearing at about v_0=0.06, increasing in amplitude and then disappearing at 0.09. Varying the IC for a little bit (about 5 percent) around the prescribed one causes the limit cycle to remain as it is. More significant variation however causes it to disappear.

We now select the operating point x_B=#33, v_0=0.08 and the special IC mentioned above so that we can characterize the limit cycle motion in detail. This time we simultaneously plot y(#81,t), y(#150,t), y(#225,t) and y(#270,t) as functions of time. The successive traces are in blue, green, red and grey. Clearly, they all oscillate together, with undiminished amplitude and identical fundamental frequency.

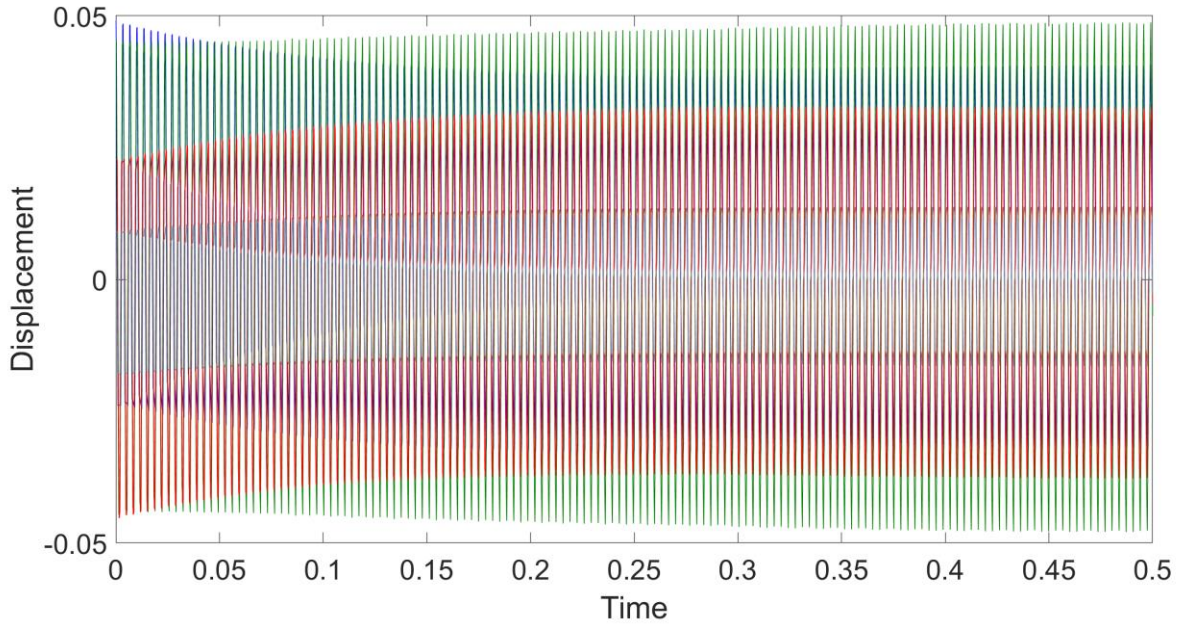

Figure 5 : Time trace of limit cycle oscillations.

Zooming in on the plot shows that the shapes of the oscillations at different points are quite different. At sites #27 and #50, the shape is close to the triangle wave while further away from the bow and closer to the end, it becomes like a cross between a square wave and a sawtooth wave.

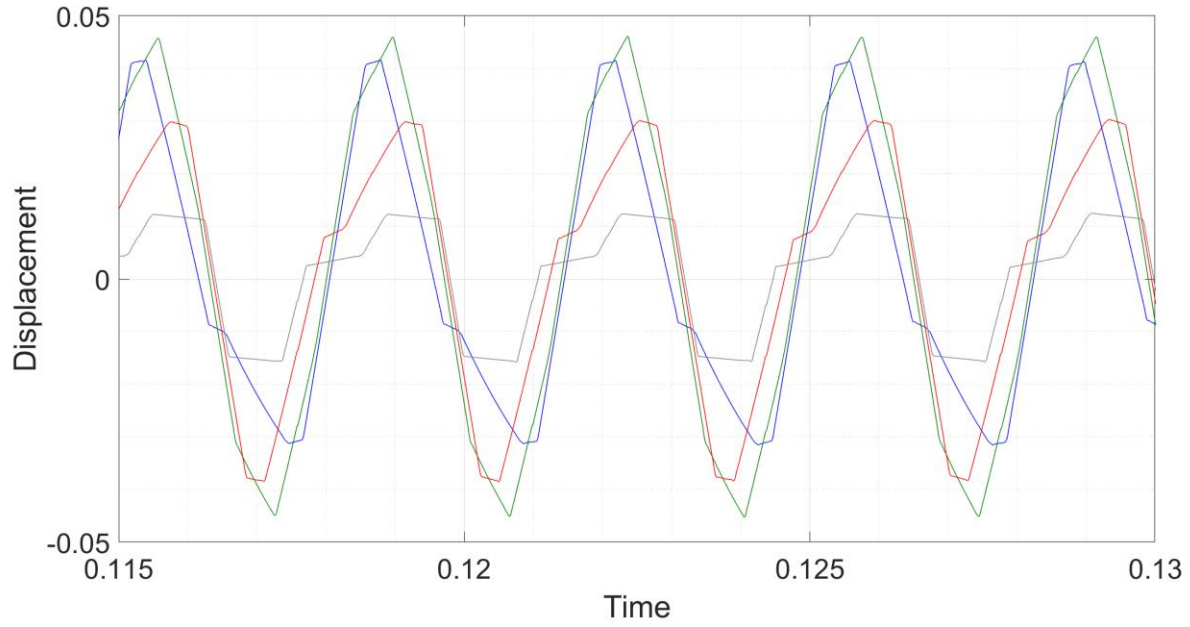

Figure 6 : Zoomed in view of the limit cycles of Fig. 5.

We now plot the velocity of the bow point as a function of time, showing only the zoomed in plot. Clearly, there are periods of stick (velocity equals 0.08 which is the bow speed) alternating with periods of slip (velocity going up and down freely, but not crossing the bow speed).

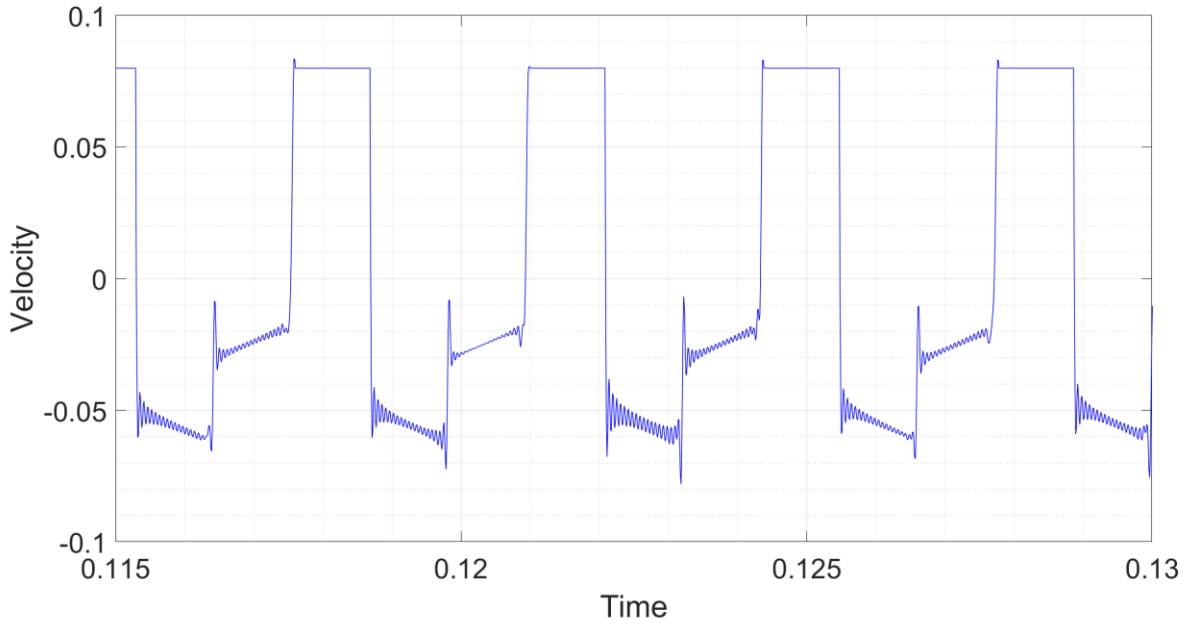

Figure 7 : Plot of velocity of the bow point as a function of time.

Finally we show the function $y(x)$ at several time points over one period. The successive time traces are in blue, green, red, grey, cyan, magenta, almost-yellow and black. At this step, we perform an analysis of convergence as the number of eigenfunctions is increased. In Fig. 8 we show superpositions of the curves with 20 and 60 spatial eigenfunctions.

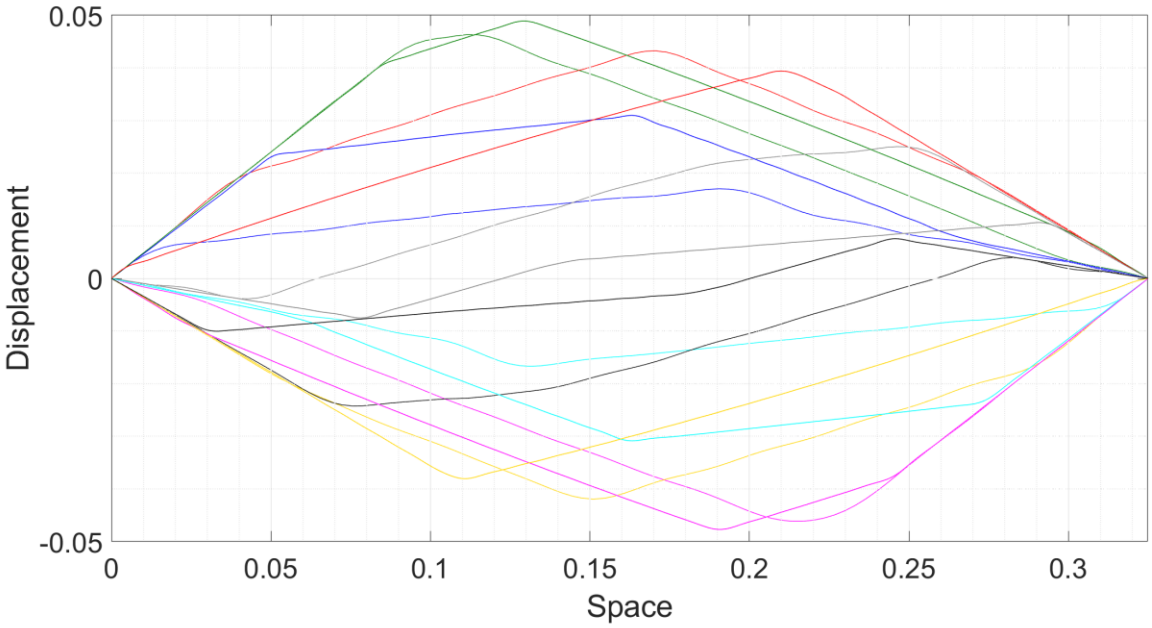

Figure 8 : Plots of the displacement y vs. x at eight intermediate points during one period of oscillation. One plot shows the situation with 20 eigenfunctions while the superimposed plot shows 60 eigenfunctions. The two are very different. The sharper lines correspond to the higher number of eigenfunctions.

Evidently the two traces are widely disparate. Increasing the number of eigenfunctions results in convergence – in Fig. 9 we superpose plots containing 200 and 600 eigenfunctions. This time the two traces cannot be distinguished. We also note that the plots for 60 eigenfunctions are very similar to those with 200 and 600.

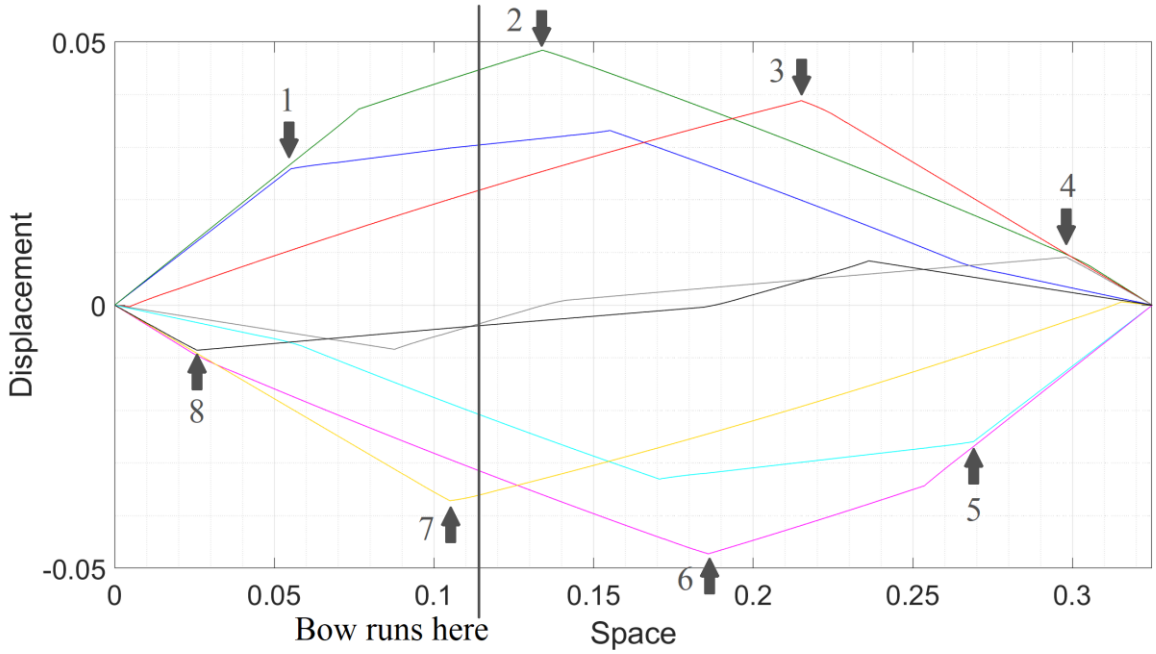

Figure 9 : Superposed plots containing 200 and 600 eigenfunctions. The two are indistinguishable.

It is noteworthy that the plots are very similar to the slow motion video of violin motion, found in Reference [16]. These plots are ample demonstration of the unique nature of PDE limit cycle oscillations in the violin string.

4. Discussion

We will now compare the present conclusions with those obtained by past authors. In Fig. 9 we can see that the profiles of the string do have a reasonably sharp corner which circulates around in a clockwise direction – this is the Helmholtz motion. This corner has been labelled by the grey arrows and a number from 1 to 8. The path of this corner is not exactly a parabola but is somewhat skewed, corresponding to the asymmetric bow point. The velocity of the bow point, Fig. 7 is indeed piecewise constant (or very close to it) – some of the oscillations are the result of Gibbs phenomenon which is ignorable. This prediction is found in all the classical works. We again note however that this motion is a solution of our equations and not a starting assumption.

For those states which don't go the limit cycle, some of them end up at the damped oscillation we saw earlier, where the bow doesn't couple. Some more

however end up at a state which the computer shows as nearly a steady state. This state is visible for any run where the bow force is too high. The time trace of any point is almost a constant and the corresponding displacement (blue) and velocity profiles (green) as functions of x are shown in Fig. 10. It appears that the computer finds in this case a virtually instantaneous transition from slip to stick and vice versa. According to the computer, the moment the string is released from this IC, the velocity of x_B becomes v_0, while the moment the bow point is dragged up a little bit, the tension difference becomes equal to μF. It is not apparent at this time whether this state is a true fixed point of the system or a computational error. The state persists upon increase of the number of eigenfunctions to very high levels. However, since it is true that excess bow force does not generate the desirable sounds from the instrument, one can probably conjecture without risk of error that even if the fixed point is spurious, the system does converge to a state which is different from the limit cycle and is musically useless.

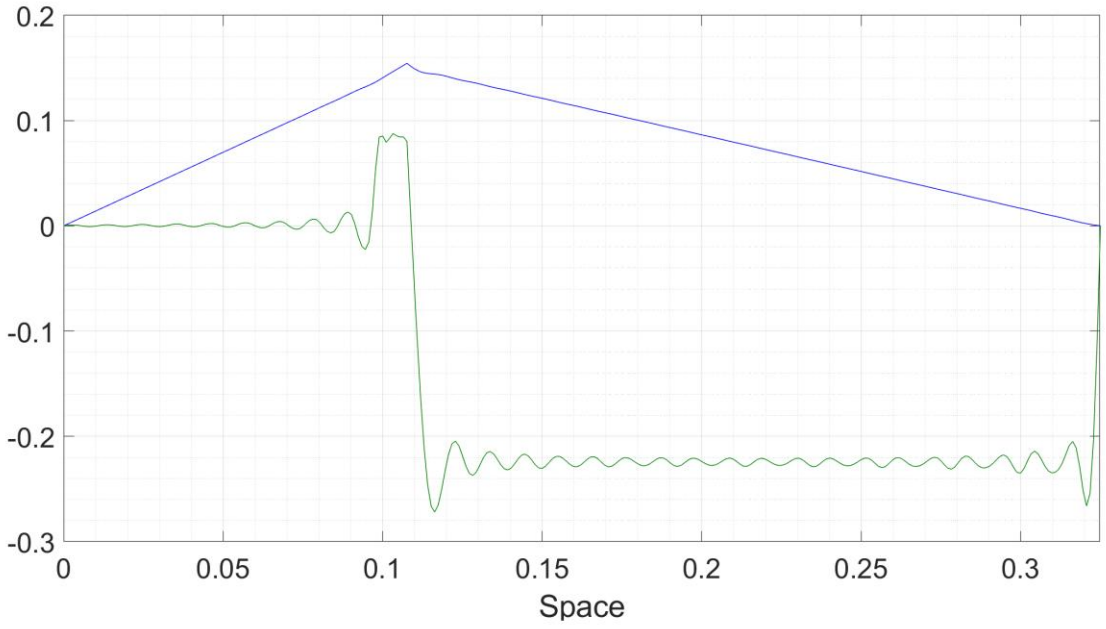

Figure 10 : Apparent pseudo-fixed point found by the computer.

The small range of parameter space where the limit cycle is stable shows why it is so difficult to play the violin properly – the margin of error in bow force, bow speed etc is quite low. The IC of the question is generated so as to produce a normal component of tension at x_B equal to μF, so that it very nearly does recreate a state where stick transitions to slip. When the string starts to be played, it is

expected that the bow will take it to such a configuration before it slips and the dynamics start off.

In Fig. 11 we present a plot of the parameter values which give rise to the limit cycle motion. Keeping everything else constant, the bow speed v_0 and the bow force F have been varied. The outcome at 40 different points has been plotted. A point is labelled in green if it leads to limit cycle oscillations, blue if it leads to damped oscillations and red if it leads to the pseudo-fixed point motion. We note that raising the force to 0.6 N kills the limit cycle motion entirely. Thus we can see that the green region is a small island surrounded by undesirable motions. This is in agreement with the fact that the violin is a difficult instrument to play. This fact however has not been brought out by any of the prior studies due to the absence of an explicit quantification of the friction term.

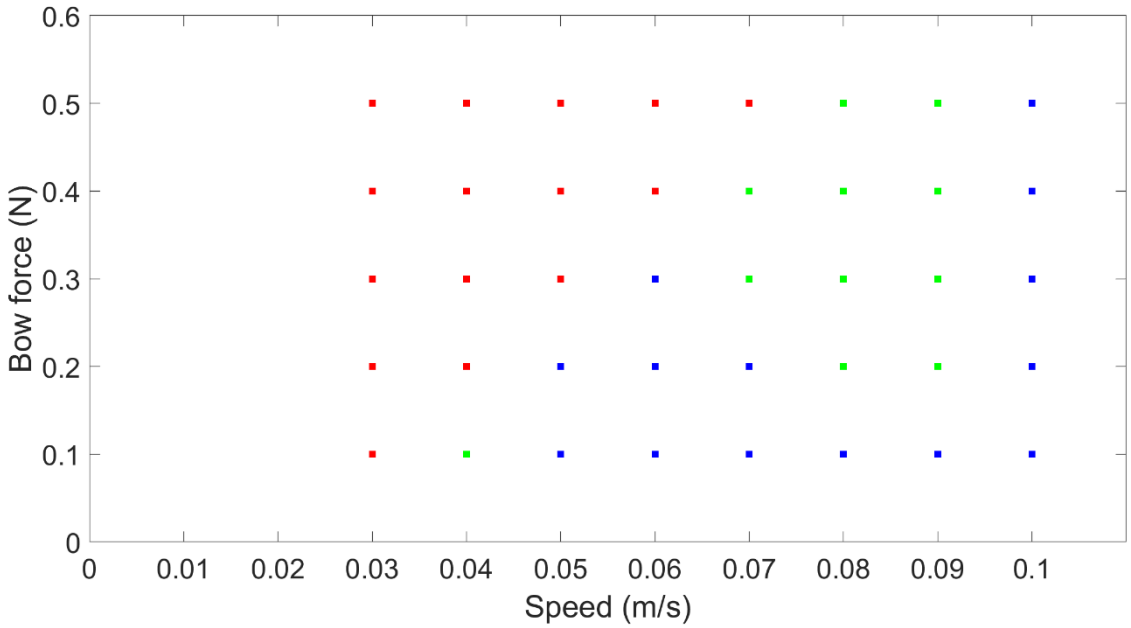

Figure 11 : Regions of parameter space showing limit cycle oscillations (green squares), damped oscillations (blue squares) and pseudo-fixed point motion (red squares).

Finally we will discuss some of the approximations and assumptions inherent in the present model. One is the assumption of μ_k=0. Replacing the zero with finite force is tedious but not conceptually complicated – in the slipping phase we have to solve not the homogeneous damped wave equation but an inhomogeneous equation with a finite force acting at x_B. Another is the boundary condition at the

ends. Instead of rigid clamping, some flexibility can be introduced by a relation like $y'(x,t)+\gamma y(x,t)=0$ at $x=0$ and $x=L$. The effect of the finite mass of the bridge (which has been neglected here) can also be factored in via insertion of a suitable term. All these however will make no qualitative difference and only minor quantitative difference to the solution which we have obtained. Hence such exercises are being reserved for future study.

Acknowledgement

I am grateful to the anonymous reviewer whose suggestions have resulted in a significant improvement in the quality of the manuscript.

References

[1] JW Strutt, the Lord Rayleigh, "*The Theory of Sound, Volume 1*" Macmillan Press, London, England (1877)

[2] CV Raman, "On the Mechanical theory of the vibrations of bowed string instruments etc." **Bulletin of the Indian Association for the Cultivation of Science** 15 (2), 243-276 (1918)

[3] JC Schelleng, "The Bowed string and the player," **Journal of the Acoustical Society of America** 53 (1), 26-41 (1973)

[4] JC Schelleng, "The Physics of the bowed string," **Scientific American** 230 (1), 87-95 (1974)

[5] RT Schumacher and J Woodhouse, "The Transient behaviour of models of bowed string motion," **Chaos** 5 (3), 509-523 (1995)

[6] J Woodhouse and PM Galluzzo, "The Bowed string as we know it today," **Acta Acustica** 90, 579-589 (2004)

[7] J Woodhouse, "The Acoustics of the violin – a review," available electronically at https://www.repository.cam.ac.uk/bitstream/handle/1810/245817/OA-1506_Violin.pdf?sequence=1

[8] JB Keller, "Bowing of violin strings," **Communications in Pure and Applied Mathematics** 6, 483-495 (1953)

[9] WI Newman, RH Rand and AL Newman, "Dynamics of a nonlinear parametrically excited partial differential equation," **Chaos** 9 (1), 242-253

(1999)
[10] SN Singh and M Brenner, “Limit cycle oscillation and orbital stability in aeroelastic systems with torsional nonlinearity,” **Nonlinear Dynamics** 31, 453-450 (2003)
[11] J Gaite, “Nonlinear analysis of spacecraft thermal models,” **ibid.** 65, 283-300 (2011)
[12] Z Monfared, Z Afsharnezhad and JA Esfahani, “Flutter, limit cycle oscillation, bifurcation and stability regions of an airfoil with discontinuous freeplay nonlinearity,” **ibid.** 90, 1965-1986 (2017)
[13] M Kuwamura and H Izuhara, “Diffusion driven destabilization of spatially homogeneous limit cycles in reaction diffusion systems,” **Chaos** 27 (3), 033112 (2017)
[14] MH Ghayesh and H Farokhi, “Nonlinear dynamics of doubly curved shallow microshells,” **Nonlinear Dynamics** 92, 803-814 (2018)
[15] JJ Stoker, “*Nonlinear Vibrations*,” Interscience Publishers, New York, USA (1950)
[16] Video available at https://en.wikipedia.org/wiki/File:Bowed_violin_string_in_slow_motion.gif